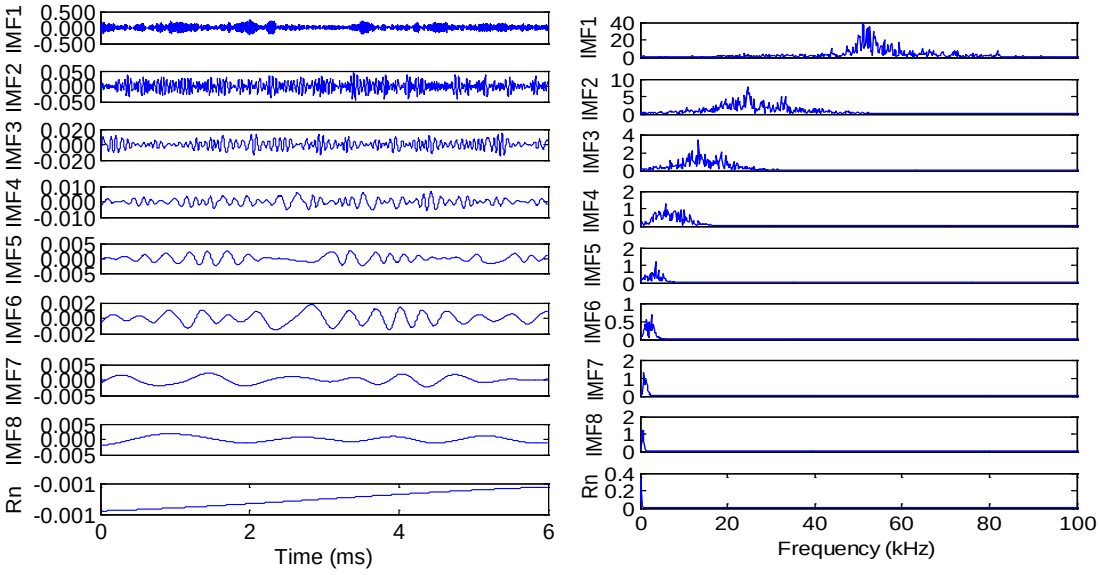

Fig. 15. EMD results of the signal from sensor 3.

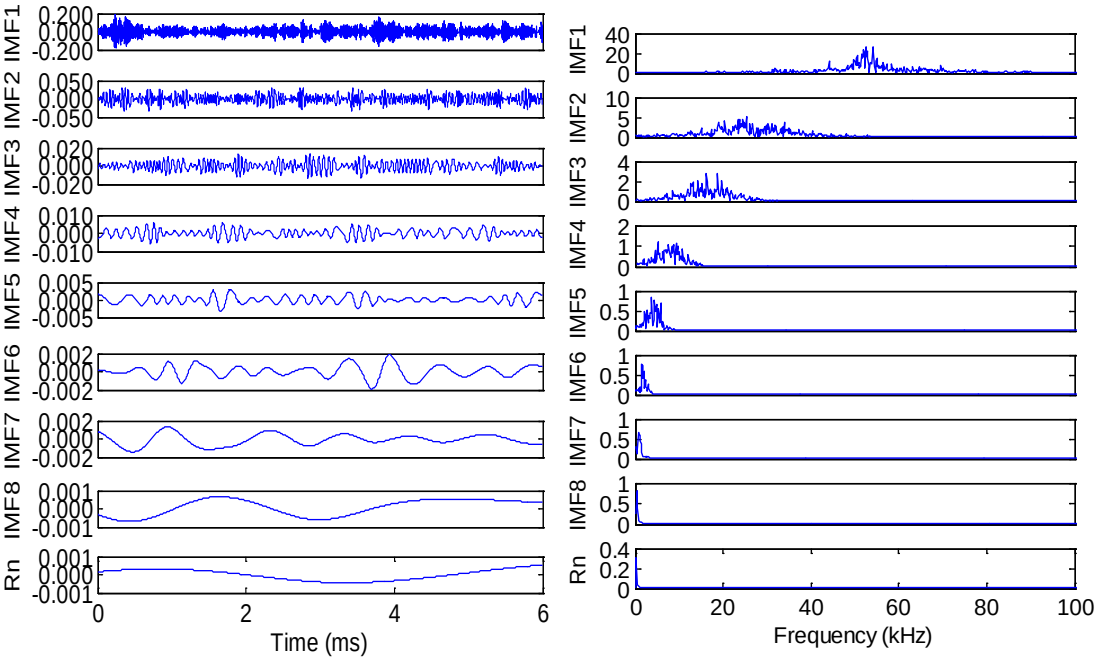

Fig. 16. EMD results of the signal from sensor 4.

It can be seen from Fig. 13-16 that eight IMF components together with a residual R_n have been generated for each AE signal received. In the time domain (plots on the left-hand-side of Fig. 13-16), the amplitudes of all the IMF components decrease by several orders of magnitudes from the highest value in IMF1 to the lowest in IMF8. In the frequency domain, the same trend is observed, i.e. IMF1 has the highest instantaneous frequency and IMF8 has the lowest instantaneous frequency. Therefore,

IMF components that contain low values of the signal magnitude and frequency can be safely ignored. Such components are more likely produced from various noise sources as indicated in Fig. 9.

Furthermore, the energy ratio of each IMF component can be calculated as follows:

$$E_{IMF\,i} = \frac{1}{N}\sum_{m=0}^{N-1} h_i(m)^2 \tag{8}$$

$$R_{IMF\,i} = \frac{E_i}{\sum_{i=1}^{8} E_i} \times 100\% \tag{9}$$

where $h_i(m)$ stands for the i^{th} IMF, N is the length of the signal, $E_{IMF\,i}$ and $R_{IMF\,i}$ represent the energy of the i^{th} IMF and its energy ratio. The results are summarized in Table 2. It can be seen that IMF1 and IMF2 contain over 98% of the energy in each signal and hence reflect the main information of the signal.

Table 2
Energy ratio of each IMF component (%).

	$R_{IMF\,1}$	$R_{IMF\,2}$	$R_{IMF\,3}$	$R_{IMF\,4}$	$R_{IMF\,5}$	$R_{IMF\,6}$	$R_{IMF\,7}$	$P_{IMF\,8}$
Sensor 1	92.46	6.37	0.91	0.17	0.04	0.02	0.02	0.01
Sensor 2	94.53	4.81	0.48	0.09	0.04	0.02	0.01	0.01
Sensor 3	94.72	4.50	0.59	0.11	0.03	0.03	0.01	0.01
Sensor 4	93.19	5.59	0.92	0.20	0.05	0.02	0.02	0.01

Therefore, a new signal is reconstructed using IMF1 and IMF2 only to represent the original signal, and the low energy components can be safely ignored:

$$S_{new}=IMF1+IMF2 \tag{10}$$

Fig. 17 shows the waveforms of the reconstructed signals.

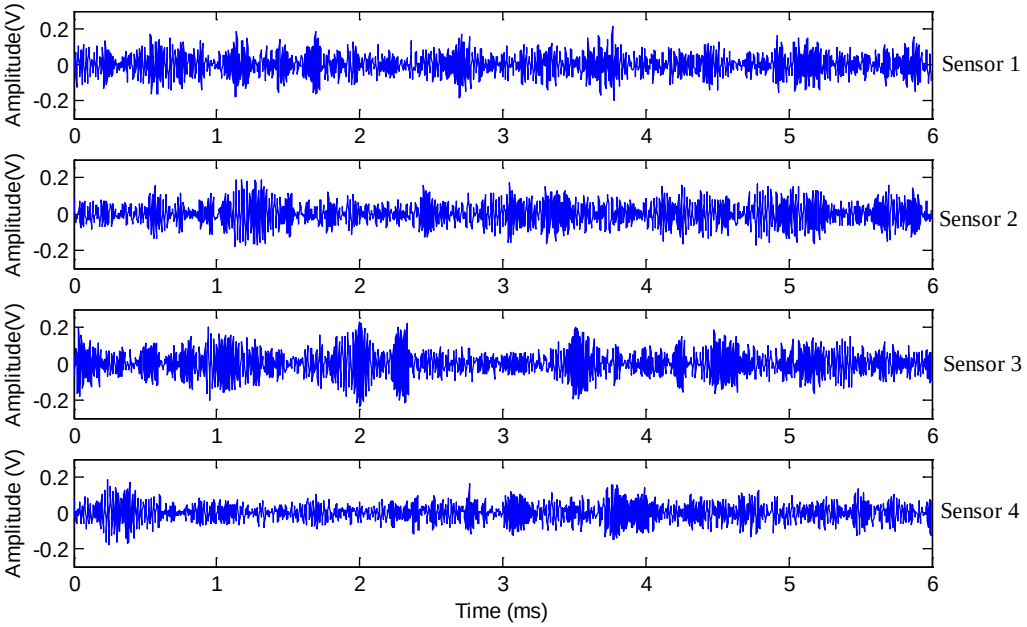

Fig. 17. Reconstructed waveforms for the AE signals.

4.4. Leak localization and error analysis

Fig. 18 shows the correlation functions between the reconstructed signals from sensor 1 and sensors 2-4 and the resulting correlation coefficients are 0.71, 0.50 and 0.48, respectively. It is suggested that sensors 1 and 2 show the strongest correlation while sensors 1 and 4 show the weakest correlation.

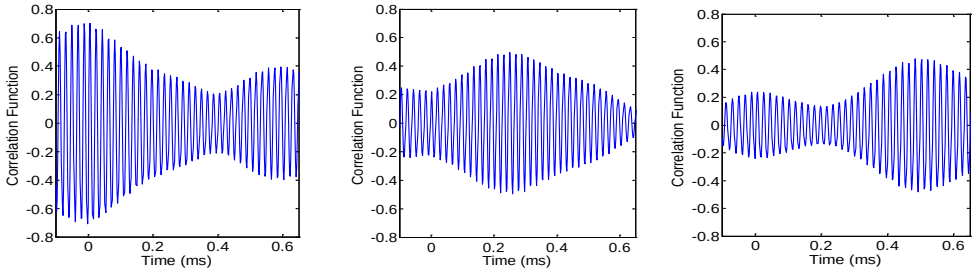

(a) Sensors 1 and 2 (b) Sensors 1 and 3 (c) Sensors 1 and 4

Fig. 18. Correlation functions between signals from sensor 1 and other sensors.

The location of the dominant peak on the time axis in the correlation function represents the time difference (Δt) between the two signals. Δt is used to calculate the location of the leak source using equation (5), together with the speeds of the AE wave obtained from the Nielsen-Hsu Pencil Lead Break Tests (Section 4.1). Table 3 lists the distance difference, Δd, and the localization errors using different pairs of sensors.

Table 3

Localization errors using different pairs of the sensors.

Sensor Pair	Correlation Coefficient	Acoustic Wave Speed (m/s)	*Time difference (ms)*	*Distance difference (m)*	*Error* (m)	Sensors Spacing (m)	Relative Error (%)
1 and 2	0.71	Longitudinal (5070)	0.002	0.01	0.01	2	0.5
		Transverse (3268)		0.01	0.01		0.5
1 and 3	0.50	Longitudinal (5070)	0.26	1.32	0.32	3	10.7
		Transverse (3268)		0.85	0.15		5
1 and 4	0.48	Longitudinal (5070)	0.49	2.48	0.48	4	12
		Transverse (3268)		1.60	0.40		10

It can be seen from Table 3 that the localization error using sensors 1 and 2 is much smaller than the other two pairs. This is because sensors 1 and 2 are symmetrical about the leak hole. Therefore the two AE signals have the same degree of attenuation and dispersion which makes them have the strongest correlation. This result reflects, to some extent, the influence of the signal attenuation and dispersion along the pipeline on the quality of the signals. With increasing asymmetry of the sensors with reference to the leak source, the correlations between the signals become weak and the localization errors increase.

Table 3 also shows that, in the case of sensors 1 and 2, the localization error is same when the transverse wave speed and longitudinal wave speed are used. However, with increasing asymmetry of the sensors' locations with reference to the leak source, i.e. sensors 1 and 3, sensors 1 and 4, the localization error is smaller when the transverse wave speed is used instead of the longitudinal wave speed. The reasons for this is that the longitudinal wave usually has the lower amplitude than the transverse wave, so it only accounts for a smaller proportion in the AE signal although its speed is higher, as seen in Fig. 9. In addition, the longitudinal wave can propagate in solid, liquid and air while the transverse wave can only propagate in the solid pipeline wall. Therefore the longitudinal wave has more energy attenuation than the transverse wave.

The results in Table 3 show a good consistency between the correlation coefficient and the accuracy of the localization, i.e. the bigger of the correlation coefficient between a pair of signals, the more accurate of the leak location result. Since the sensor array will be installed in the industrial processes, a data fusion method based on correlation coefficient of the signals should be a reasonable and effective approach to accurately localize the leak source. The weight coefficient u_i and localization error ε_i can be

calculated using equations (11) and (12), respectively, as follows:

$$\varepsilon = \sum_{i=1}^{3} u_i \varepsilon_i \tag{11}$$

$$u_i = \frac{r_i}{\sum_{i=1}^{3} r_i} \tag{12}$$

where r_i and ε_i represent the correlation coefficient and the error used the i^{th} pair of the AE sensors, respectively.

This data fusion method fully considers the reliability of measurement results from multi sensors. The localization error is 4.5% when the transverse wave speed is used and 6.8% when the longitudinal wave speed is used. The results show that the technique has a good performance in the leak localization.

5. Conclusions

In this paper investigations have been carried out experimentally on the potential use of low frequency and narrow band AE sensors for the localization of accidental CO_2 leak from long distance transportation pipelines. The influences of signal attenuation and dispersion have been effectively minimized using the empirical mode decomposition technology which has shown a good performance in processing the non-linear and non-stationary AE signals. Newly reconstructed AE signals, based on the main energy components of the IMF, i.e. IMF1 and IMF2 (up to 98%), have been employed to predict the location of the leak through cross-correlation of the reconstructed signals. There is a good consistency between the correlation coefficient and the accuracy of the leak localization. When the two AE sensors are symmetrically installed about the leak source, the maximal correlation coefficient has been obtained and the localization error is less than 1%. With an increasing asymmetry of the sensor installations with respect to the source of the leak, the correlation between the signals becomes weak and the localization error increases. Furthermore, the speeds of the transverse and the longitudinal waves are measured using the Nielsen-Hsu Pencil Lead Break Test. These speeds have been used to determine the location of the leak. It is observed that the localization errors are smaller when the transverse wave speed is used. Finally, a data fusion method based on the correlation coefficient has been employed. The results have demonstrated that the system gives a localization error of 4.5%. In summary, low frequency and narrow band AE sensors together with empirical mode

decomposition and signal reconstruction have a good potential to localize leaks from a long distance CO_2 pipeline.

Acknowledgement

The authors wish to acknowledge the Chinese Ministry of Science and Technology (MOST) and the Chinese Ministry of Education for providing financial support for this research as part of the 111 Talent Introduction Projects (B13009) at North China Electric Power University. This work was also supported by the Fundamental Research Funds for the Central Universities (No. 2014XS40). Xiwang Cui would like to thank the China Scholarship Council for offering an academic exchange grant for his visit to the University of Kent.

References

[1] S. M. Benson, T. Surles. Carbon dioxide capture and storage: An Overview with emphasis on capture and storage in deep geological formations, Proceedings of the IEEE, 2006, 94(10), pp.1795-1805.

[2] J. Gale, J. Davison. Transmission of CO_2 safety and economic considerations. Energy, 2004, 29(10), pp.1319-1328.

[3] G. J. Zhang, Y. P. Li, Q. B. Li. A miniaturized carbon dioxide gas sensor based on infrared absorption. Optics and Lasers in Engineering, 2010, 48(12), pp.1206-1212.

[4] A. Somov, A. Baranov, D. Spirjakin, A. Spirjakin, V. Sleptsov, R. Passerone. Deployment and evaluation of a wireless sensor network for methane leak detection. Sensors and Actuators A: Physical, 2013, 202, pp.217–225.

[5] S. Huang, W. Lin, M. Tsai, M. Chen. Fiber optic in-line distributed sensor for detection and localization of the pipeline leaks. Sensors and Actuators A: Physical, 2007, 135(2), pp.570-579.

[6] Z. Guan, M. Lewander, R. Gronlund, H. Lundlerg, S. Svanberg. Gas analysis within remote porous targets using LIDAR multi-scatter techniques. Applied Physics B: Lasers and Optics, 2008, 93(2), pp.657-663.

[7] I. M. Perez de Vargas-Sansalvador, C. Fay, T. Phelan, M. D. Femandez-Ramos, L. F. Capitan-Vallvey, D. Diamond, F. Benito-Lopez. A new light emitting diode-light emitting diode portable carbon dioxide gas sensor based on interchangeable membrane system for industrial applications. Analytica Chimica Acta, 2011, 699(2), pp. 216-222.

[8] J. A. Hogan, J. A. Shaw, R. L. Lawrence, J. L. Lewicki, L. M. Dobeck, L. H. Spangler. Detection of leaking CO_2 gas with vegetation reflectances measured by a low-cost multispectral imager. IEEE Journal of Selected Topics in Applied Earth Observations and Remote Sensing, 2012, 5(3), pp. 699-706.

[9] P. Murvay, I. Silea. A survey on gas leak detection and localization techniques. Journal of Loss Prevention in the Process Industries, 2012, 25(6), pp. 966-973.

[10] G. Zhang, Y. Li, Q. Li. A miniaturized carbon dioxide gas sensor based on infrared absorption. Optics and Lasers in Engineering, 2010, 48(12), pp. 1206-1212.

[11] V. L. Kasyutich, P. A. Martin. A CO_2 sensor based upon a continuous-wave thermoelectrically-cooled quantum cascade laser. Sensors and Actuators B: Chemical, 2011, 157, pp. 635-640.

[12] V. R. Lakkaraju, X. Zhou, M. E. Apple, A. Cunningham, L. M. Dobeck, K. Gullickson, L. H. Spangler. Studying the vegetation response to simulated leakage of sequestered CO_2 using spectral vegetation indices. Ecological Informatics, 2010, 5(5), pp.379–389

[13] S. J. Martin, G. C. Frye, J. J. Spates, M. A. Butler. Gas sensing with acoustic devices. IEEE Ultrasonics Symposium Proceedings, 1996, 1, pp. 423-434.

[14] R. K. Miller, A. A. Pollock, D. J. Watts, J. M. Carlyle, A. N. Tafuri, J. J. Yezzi. A reference standard for the development of acoustic emission pipeline leak detection techniques. Non-Destructive Testing and Evaluation (NDT & E) International Journal, 1999, 32(1), pp. 1-8.

[15] K. Adefila, Y. Yan. A compendium of CO_2 leakage detection and monitoring techniques in carbon capture and storage (CCS) pipelines. EUROCON, 2013 IEEE, pp. 1328-1335.

[16] A. Mostafapour, S. Davoudi. Analysis of leakage in high pressure pipe using acoustic emission method. Applied Acoustics, 2013, 74, pp.335-342.

[17] [On-line] Soundwel Technology, Acoustic emission technology application, http://wenku.baidu.com/link?url=fDIrbgs2br4T4yOpuUPUjOCfruLJjtMiBysC21TbD9a_1vkZGR2M5iDYHBrsJo-WmoZKl84idYjKiiBbStKiRqQSmLfAMtqjUC82G3xLAmW. Accessed 2015/3/24.

[18] W. H. Prosser, K. E. Jackson, S. Kellas, B. T. Smith, J. Mckeon, A. Friedman. Advanced waveform-based acoustic emission detection of matrix cracking in composites. Materials Evaluation, 1995, 9, pp. 1052-1058.

[19] P. Wilcox, M. Lowe, P. Cawley. The effect of dispersion on long-range inspection

using ultrasonic guided waves. Non-Destructive Testing and Evaluation (NDT & E) International Journal, 2001, 34, pp. 1-9.

[20] B. Liu, S. Riemenschneider, Y. Xu. Gearbox fault diagnosis using empirical mode decomposition and Hilbert spectrum. Mechanical Systems and Signal Processing.2006, 20(3), pp. 718-734.

[21] Z. Shen, N. Feng, Y. Shen, C. Lee. A ridge ensemble empirical mode decomposition approach to clutter rejection for ultrasound color flow imaging. IEEE Transactions on Biomedical Engineering, 2013, 60(6), pp. 1477-1487.

[22] D. Huang, J. Zhao, J. Sun. Practical implementation of Hilbert-Huang transform algorithm. Acta Oceanologica Sinica, 2003, 22(1), pp. 1-14.

[23] Y. A. Khulief, A. Khalifa, R. B. Mansour, M. A. Habib. Acoustic detection of leaks in water pipelines using measurements inside pipe. Journal of Pipeline Systems Engineering and Practice, 2011, 3(2), pp. 47-54.

[24] S. Li, Y. Wen, P. Li, J. Yang, L. Yang. Determination of acoustic speed for improving leak detection and location in gas pipelines. Review of Scientific Instruments, 2014, 85(2), pp. 024901-11.

[25] X. Qian, Y. Yan. Flow measurement of biomass and blended biomass fuels in pneumatic conveying pipelines using electrostatic sensor-arrays. IEEE Transactions on Instrumentation and Measurement, 2012, 61(5), pp. 1343–1352.